7.3

AN EXAMINATION OF THE PERFORMANCE OF TWO HIGH-RESOLUTION NUMERICAL MODELS FOR FORECASTING EXTENDED SNOW BANDS DURING THE DTC WINTER FORECAST EXPERIMENT

Edward J. Szoke[1] and Steven E. Koch[2]
NOAA Research–Forecast Systems Laboratory, Boulder, Colorado
[1]Collaboration with the Cooperative Institute for Research in the Atmosphere (CIRA), Fort Collins, Colorado
[2]Also affiliated with the Developmental Testbed Center (DTC), Boulder, Colorado

David Novak
NOAA National Weather Service Eastern Region Headquarters, Bohemia, New York

1. INTRODUCTION

Two high-resolution numerical models were run daily on the CONUS scale for the 2005 winter season at the Developmental Testbed Center (DTC) during the DTC Winter Forecast Experiment (DWFE). The models had different dynamic cores of the Weather Research and Forecasting (WRF) model, one using the NCAR Advanded Research WRF model (hereafter called the ARW), and the other the NCEP Nonhydrostatic Mesoscale Model (NMM), and both were run with a horizontal grid resolution of 5 km (Bernadet et al. 2005). They were initialized at 0000 UTC, using the Eta (hereafter NAM) initialization, with forecasts out to 48 h. The high resolution enabled the models to be run without using a convective parameterization scheme. The objectives of this exercise include determining the potential value of running a high-resolution model for winter weather forecasting, whether there is improvement over the current operational models, and whether they can resolve small scale features (Koch et al. 2005). Both deterministic (Demirtas et al. 2005) and subjective evaluations are important to determining the value of the forecasts. Subjective evaluations were collected in real-time during the forecast exercise using an online form, and are discussed in Koch et al. (2005). In this paper we examine the most basic aspect of a winter forecast, the predicted snowfall, keying on events east of the Rockies that produced a significant extended area of snowfall. For all the cases we compared the forecast snowfall and snow precipitation from the ARW and NMM to what was observed, and also to forecasts from the operational models, the NAM and GFS. Two of the cases are used to more closely examine whether the high-resolution models could predict smaller scale aspects of the storm, such as embedded bands of snow, timing and evolution.

It is apparent that a model with a 5-km horizontal grid resolution and explicit convection can predict detail for certain situations that is not possible with the current operational model suite. An example of this would be convective cells within narrow lake effect snowbands (Koch et al. 2005). High-resolution models can also better resolve terrain features. While these situations are important to forecasters, in this paper we wanted to address the more general types of winter storms that can produce widespread areas of snowfall that affect several National Weather Service (NWS) Weather Forecast Offices (WFOs). With this in mind we only considered snowstorms east of the Rocky Mountains, to avoid terrain effects, and avoided lake effect-only situations. For all the events we first addressed simply how well the high-resolution models did in predicting snowfall, and whether there was any improvement over the current operational models. A listing of all the events with a few characteristics is given in Table 1. While the 2004-2005 winter was an exceptional one for the Northeast, it was actually a rather active winter overall across the CONUS, and we were able to save a number of cases that met our criteria.

Predicting the general amount of snow and approximately where it will fall is certainly among the highest priorities for winter weather forecasters. It is also important to predict when the snow will begin or end and whether there will be embedded regions of locally higher snow accumulations. Often bands of heavier snows develop in environments with frontogenesis in the presence of weak moist symmetric instability (as noted also by Novak et al. 2004). In general, operational models in the past have not been able to predict such specific banded structures, and forecasters have had to determine if conditions supportive of banded precipitation were present to infer that they might occur. Even then, however, it was difficult to know specifically where the band would develop, or if there would be multiple bands. With the models run during the DWFE it was hypothesized that such bands of snowfall might be predicted explicitly, and this is examined in the cases.

2. METHODOLOGY

Making a comprehensive subjective evaluation of the large number of cases proved to be a daunting task, for example, just in determining how much snow actually fell and when it occurred. For many of the events WFOs compiled excellent post-storm snowfall maps, which, when combined with

Corresponding author address: Ed Szoke, NOAA/OAR/FSL, R/FS1, 325 Broadway, Boulder, CO 80305; e-mail: Edward.J.Szoke@noaa.gov

Table 1 . Key characteristics of 2005 DWFE winter cases				
Date	Type of system	Snowfall (inches)	Snow extent	Highlights
18–19 Jan	Alberta Clipper	1 to 2	area-ne MN to nrn OH	some transient nnw-sse bands
19–21 Jan	Alberta Clipper	1 to 6	band-ND to VA/NC	ne-sw single to multiple bands
21–22 Jan	Alberta Clipper	4 to 10	ND/SD to PA/NY	embedded ~e-w bands at times
23–24 Jan	Nor'Easter	6 to 36	DC to New England	terrain effects seen in hi-res runs
25–26 Jan	Alberta Clipper	2 to 6	nrn MN/WI - Northeast	two ~e-w bands over Northeast
28–30 Jan	~E-W band w/o sfc low	3 to 16	KS/OK to Mid Atlantic	8-16 in narrow e-w band in KS
1–3 Feb	~E-W band w/o sfc low	1 to 5	nw TX to Mid Atlantic	extensive 1-5 in area
6–7 Feb	Stalled cold front	2 to 7	KS to WI	snow band at back edge of pcpn
7–9 Feb	~E-W band w/o sfc low	1 to 7	KS to Ohio Valley	widespread but band ern KS
10–11 Feb	Nor'Easter	3 to 24	Northeast	rain vs snow issue in Northeast
14–16 Feb	~E-W band w/o sfc low	1 to 4	NE; IL to nrn NY	wrn NE band, then area to east
19–21 Feb	Surface low	1 to 5	ND/SD to IN	several ~e-w bands
22–24 Feb	~E-W band w/o sfc low	1 to 5	KS to Mid Atlantic	~e-w bands from MO to Ohio
1 Mar	Nor'Easter	4 to 24	wrn NC to ME	signifcant band in New England
8–9 Mar	Alberta Clipper	1 to 2	ND to srn MO	extended band of light snowfall
10–12 Mar	Alberta Clipper	1 to 4	ne ND to NY/PA	relatively disorganized structure
15–16 Mar	Alberta Clipper	1 to 4	ne ND to MI	some ~e-w banding
17 Mar	Alberta Clipper	1	nrn IA to nrn IL	narrow but distinct ~e-w band
18–19 Mar	Alberta Clipper	6 to 23	nrn IA, srn MN to WI	narrow very heavy band

radar data to determine when the snow began and ended, were extremely useful. Another source for snowfall is from the National Operational Hydrologic Remote Sensing Center (NOHRSC, on the web at http://www.nohrsc.nws.gov). This comprehensive site not only has maps of snowfall but also snow precipitation, which was useful to directly compare to model quantitative precipitation forecasts (QPF). An additional site useful for determining 24-h precipitation is the NOAA National Precipitation Verification Unit (NPVU), at http://www.hpc.ncep.noaa.gov/npvu/index.shtml.

In assessing the cases the above sites were used to determine both the observed snowfall and the water equivalent. We did not archive snowfall forecasts from the operational models, so the QPF forecasts were verified, with equivalent snow estimated by an approximate 10:1 ratio (or another ratio if data allowed us to compute it) and compared to archived snow maps, which at times displayed greater detail than the other sources. For the NMM and ARW models, QPFs were available but also snowfall forecasts were archived. These forecasts were available from the NWS Advanced Weather Interactive Processing System (AWIPS), applying a relatively simple snow algorithm. The AWIPS algorithm uses thickness values to adjust from the basic 10:1 ratio, which generally works reasonably well in many situations east of the Rockies, but it performs poorly in situations where maritime influences are significant, most notably in the Pacific Northwest, and at times near the East Coast.

Products from the ARW and NMM were archived from images generated on FX-Net (Madine et al. 2002), a PC-based client developed at FSL that replicates many of the properties of AWIPS, but uses a relatively low bandwidth connection. We concentrated on archiving QPF and snow accumulation forecasts, as well as appropriate cross sections and plan view fields to help determine the important dynamic meteorological features. Derived forcing fields from high-resolution models can be quite noisy, as explained in Koch et al. (2005b), and for comparison "verification" fields were saved from AWIPS using the NAM on an 80-km grid. Precipitation fields at 12-h intervals from the NAM and GFS were saved from the NCEP web site located at http://www.nco.ncep.noaa.gov/pmb/nwprod/analysis. Other ARW and NMM model fields, including model and observed reflectivity, were archived by the Joint Office for Science Support (JOSS, at http://www.joss.ucar.edu/).

To examine whether the ARW and NMM could predict smaller scale aspects of the various events, we chose a small subset from all the cases in this paper. A relatively new model field of reflectivity, not available from the current operational models, was used to compare to observed radar reflectivity for the two case studies.

3. OVERVIEW OF THE CASES

As seen in Table 1, the storms chosen produced an extended swath of snow at least 500 km long, but more often substantially longer (1500 km). Typically the snow fell in a relatively narrow band, perhaps 100 to 300 km wide, or in bands of snow. A number of the events saved were associated with long-track "Alberta Clipper" type storms, typified by a weak surface low tracking out of Canada along a stalled cold front across the northern section of the CONUS. Other cases had considerably less organized surface lows but a well-defined jet streak and low to mid-level organized warm advection (labelled “~E-W band w/o sfc low” in Table 1). Some of these more innocuous storms can be especially tricky to predict, and although they do not produce the hefty snows of a well-developed Nor'Easter, they can result in an extensive band of 1 to 4 in type snowfall affecting a number of WFOs and producing widespread travel problems. A brief summary for each of the cases is given in Table 2.

Table 2. Summary of Cases

Date	Forecast Summary
18–19 Jan	Some overprediction of snowfall by the NMM and ARW for this weak system.
19–21 Jan	Some overprediction by NMM and ARW, more so NMM. NAM similar to ARW. GFS amounts ok, but area too broad. All models miss the southern OH/IN snowfall max of ~6 in, tending to be too far north at 24–36 h. Underprediction of northern NC snow, except by GFS.
21–22 Jan	Major system for Midwest to Ohio Valley into NY/PA; good overall forecast by ARW/NMM, and also NAM. NAM most similar to ARW. No GFS saved for this case.
23–24 Jan	Nor'Easter with impressive snowfall. Overall good forecasts, strong terrain forcing noted in western New England and eastern NY in the ARW and NMM.
25–26 Jan	Disorganized structure until Clipper reaches the Northeast, then 3 ~east-west bands in eastern NY into southern New England. ARW does best with these in 36 h forecast; however no real improvement seen in the 12 h forecasts from the next run.
28–30 Jan	Extensive ~east-west snow system all the way from OK/KS to the Midwest and Ohio Valley then to the Mid-Atlantic. Two periods where a well-defined band present, in KS on 28th and nrn IL to nrn OH on 29th. Focus on narrow east-west band of 8–16 in snow in KS. All 36–48 h forecasts failed to predict such an intense band, and to some extent the overall area of snow, with ARW the best. Next run (12–24 h forecasts) did better in capturing the overall area of snow in KS/OK, but none correctly forecast an embedded heavy band. NMM and ARW did forecast a snow band in the approximate area in KS but underforecast amounts.
1–3 Feb	Extensive snow area but less than late Jan. event with generally 1–5 in. Models tended to miss the max snowfall in OK, then were too far south with the sharp northern edge in the Ohio Valley, though some aspects were handled well. Slight edge to the ARW, and overall the ARW/NMM had more detail than the NAM or GFS.
6–7 Feb	Stalled/slow-moving cold front with large area of precipitation near and on the cold side of the front, with snow on the back (west) edge in a relatively narrow band from KS to IA/WI, with a zone >6 in, mainly in NE. ARW and NMM do a little better than the NAM, which was too far south with the nw edge of the precipitation; actual band just between ARW and NMM solutions, with the snow amounts from the ARW/NMM generally good.
7–9 Feb	500-mb shortwave trough moving east out of Rockies but no well-defined surface low, instead more of an overrunning situation. Best snowband occurs in eastern Kansas on 8 Feb and results in 4–7 in of snow; otherwise rather disorganized with widespread 1–3 in accumulations but sharp southern cutoff from MO eastward. Mixed results; best handling of eastern Kansas max is by the ARW, but overall best forecasts are with the NMM and NAM.
10–11 Feb	Nor'Easter develops but temperatures warm enough for rain/snow issues in the southern half of New England, with big snows northern half. Issues with simple AWIPS snow algorithm vs using model physics to determine snow vs rain; direct model forecast from the ARW is quite a bit better. ARW/NMM appear to overforcast orographic snow in northern New England.

Table 2 (continued).	
Date	Forecast Summary
14–16 Feb	The initial band of snow in western Nebraska was not predicted very well by any of the models. Snow from IL eastward was forecast, though amounts in the ARW/NMM were somewhat excessive, especially the NMM, with NAM more in line with correct snowfall.
19–21 Feb	Surface low moves out of the Central Rockies into the Midwest with area of snow to the north and east of the low, organized frequently into ~east-west bands. Heaviest snows fell in MN to SD, but large area of light snow. Overall models did a good job, and the ARW/NMM were similar to the NAM. All tended to somewhat overpredict the snow over SD.
22–24 Feb	Weak system that spreads a streak of snow eastward from KS eventually to the Mid-Atlantic, before system develops a surface low off the East Coast. Initial 1–2 in narrow band in KS was not well forecast by any of the models. Next main area of snow from southern MO eastward across the southern Ohio Valley, with a sharp northern cutoff to the 1–4 in snowfall. The northern extent of the snow in the Ohio Valley proved tricky for the models, as both the ARW and NMM, and the NAM (and to a lesser extent the GFS) tended to forecast the northern edge of the snow too far to the south.
1 Mar	Low develops off GA coast and moves up the East Coast producing significant snows from the Mid-Atlantic region through the Northeast. Generally good forecasts except by the GFS. ARW/NMM captured banding but tended to overdo the orographic effects in the Northeast.
8–9 Mar	A rather weak Alberta Clipper slides southeastward from the Dakotas to northern Arkansas leaving a lengthy swath of light snow accumulations of generallly under 2 in. No NMM available. ARW has a good overall forecast, with the NAM close except that it misses the snow in southern MO. The GFS better overall than the NAM for this case.
10-12 Mar	Next Clipper system moves in a more typical fashion and is stronger with a long stretch of 1–4 in snows. Mostly disorganized without much banded precipitation. ARW/NMM similar to NAM and all produce good forecasts, except for being too slow to spread the snow eastward. The GFS forecast generally not as good.
15-16 Mar	Weak surface low tracks out of Canada and produces a swath of light snow from ne ND to MI, as the first of 3 events in this area in 4 days. No GFS archived. NAM, NMM and ARW are similar: decent forecasts except all do not produce enough snow in WI.
17 Mar	Not a big case, but an interesting streak of snow develops in the Midwest with a very narrow band of 1 in accumulations. 36 h forecasts tended to be too slow to start the snow, with a band appearing after 12 UTC/17 Mar, although the ARW did develop a weaker band before then, and the GFS also had a small area of light precipitation. 12 h forecasts from the next run all show improvement, with the ARW/NMM having better detail.
17–19 Mar	A record-setting storm with over 20 in of snow in a narrow band across southern MN and far northern IA into WI. Very sharp northern cutoff to the snow east-west across Minneaspolis. Strong warm advection at low levels concentrated by a small-scale but deepening wave associated with an Alberta Clipper system. Main snow fell in an east-west band associated with the warm advection, but there were other bands to the south oriented perpendicular to the main band that may have been associated with gravity waves forced by a jet streak. Overall all models show skill in forecasting a concentrated area of snow at 48 h, and the shorter term forecasts are consistent in focusing on the area of southern Minnesota.

It became apparent as the cases were evaluated that the accumulated precipitation forecasts in areas of snow from the NAM were difficult to beat, as seen in some of the comments in Table 2. This table shows there are instances where the ARW and NMM provided some details in the snow accumulation forecasts that were better than the NAM, but in other instances, the NAM actually made as good or even a better forecast. We will demonstrate with two case studies that there are other ways in which the high-resolution models provided important information to forecasters that was not available from the NAM, but in terms of overall snow accumulation, the differences between the NAM and the high-resolution models, *for the types of systems considered here*, are not substantial. Possible reasons for this include the following:

- The NMM and ARW were initialized using the NAM;
- The NAM is run at a relatively high horizontal grid resolution of 12 km, so is able to capture the overall snowfall distributions on the scales considered here;

- Differences between the NAM and the ARW/NMM are more likely to be found where convection is an important contribution to the precipitation, since at convective scales the difference between 5 and 12 km becomes more significant, and also the NAM uses a convective parameterization scheme while the ARW and NMM do not. In the winter events considered here (as opposed, for example, to lake effect snow bands) convective elements were not apparent in many of the cases.
- Accumulated snowfall over some period of time (12–24 h) blends spatially discrete details about bands at instantaneous times into a temporally smoother field.

Next the cases are examined by the type of system, as noted in Table 1.

3.1 *Alberta Clipper cases*

As seen in Table 1, this was the most common category of storm system archived during the DWFE. These systems typically left an extended swath of snowfall from the Northern Plains or Upper Midwest, as they exited Canada, sometimes all the way to the Northeast, as shown in Fig. 1. In a few of the cases, the storm would intensify off the coast to form a Nor'Easter. The 21–22 Jan storm was of this type, and the strongest Clipper system in terms of a surface low, producing heavy amounts of snow in the Midwest and Ohio Valley before the storm evolved into the major Nor'Easter of 22–23 Jan as it redeveloped off the coast. In general, though, most of the Clipper systems were characterized by an extensive swath of relatively light snowfall, in the 1–4 in range, and usually, but not often, a distinct though usually weak surface low. The typical dynamic forcing for snowfall involved low to mid-level warm advection and an upper level jet streak. Usually one could find a shortwave trough at the 500 mb level that dropped out of Canada and was associated with each system, and indeed, this was a characteristic for placing some of the less obvious cases (that might have fallen into the category discussed in Section 2.2) into the Alberta Clipper category. A well-defined zone of frontogenesis at and below 700 mb was typically seen for the cases with a more narrow swath of snow. Radar reflectivity usually revealed some banded structure but often it was a transient feature, with a broader area of more disorganized snow at other times.

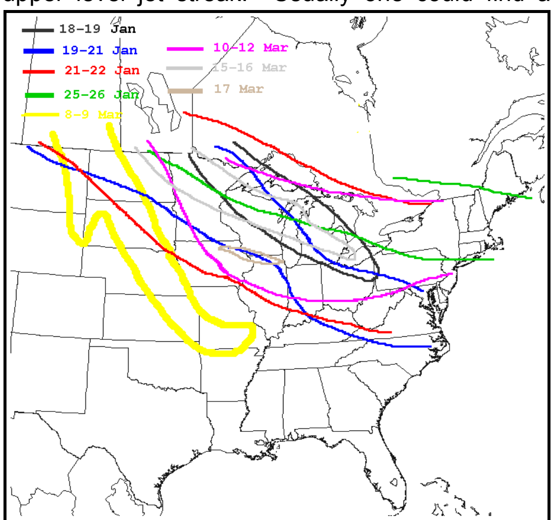

Fig. 1. Outlines of the swaths of measurable snowfall for the various Alberta Clipper systems listed in Table 1.

The most impressive exception for this type of system in terms of snowfall was the 18–19 Mar storm, which produced record-breaking snowfall in a relatively narrow swath across southern Minnesota, extreme northern Iowa, and into southwestern Wisconsin. This storm is described in detail in Section 4. Even the more typical Clipper events, though, were important for operational forecasters, with challenges often found in determining timing of the snowfall and whether amounts would be on the order of an inch or at the more significant 2–5 in range.

For the typical Alberta Clipper cases there was some tendency for the high-resolution models (ARW/NMM) to overforecast the amount of snow at times, though this was not a characteristic of all the cases. There were timing errors that both the operational and high-resolution models shared, most notably in the 36-h forecasts for the 15–16 and 17 Mar cases, where snow developed eastwards more quickly than any of the models forecast. The 17 Mar case was a particularly narrow (~50 km) band of light (~1 in) snow, and for this case the ARW and NMM did have somewhat better forecasts than the NAM, with the ARW the earliest (and therefore most correct) to develop the snow. Overall, though, except for a band of snow in southern Ohio/Indiana not forecast by any model for the 19–21 Jan case, no real "busts" were seen for the Alberta Clipper cases for either the ARW and NMM or the NAM models.

3.2 *~East-west bands without a distinct surface low*

This category had the second highest number of the cases. As seen in Fig. 2, an extended swath of snow aligned more east to west and located across the mid-CONUS (rather than northern half of the CONUS in most of the Alberta Clipper cases) was the general characteristic of the snowfall distribution. Typically the swath of snow would develop well behind (north of) a stalled cold front lying across the southern states, with little if any notable surface low present. Eventually a surface low could develop as the system spread closer to the Mid-Atlantic region, sometimes leading to a signifcant coastal low, as in the 22–24 Feb event. Upper level features included an often extensive jet eminating from the Southwest,

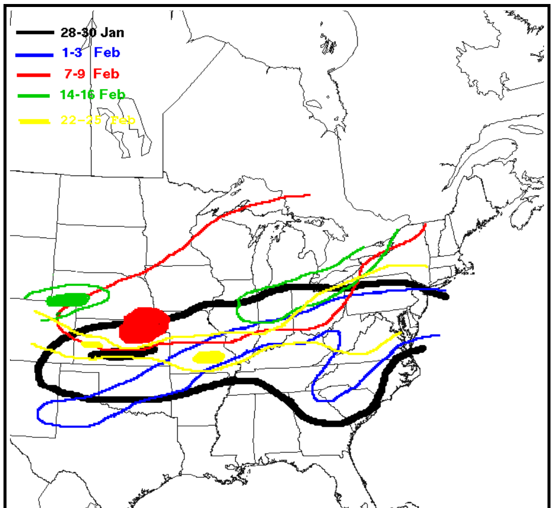

Fig. 2. As in Fig. 1, but for cases lacking any distinct surface low (labeled "~E-W band w/o sfc low" in Table 1). Shaded areas show the locations of the heaviest snows.

perhaps with an embedded jet streak, and could include a definable shortwave trough at 500 mb. Below 500 mb, warm air advection was present, typically with a well-defined area of upglide of warm and moist air identified on isentropic analyses as starting south of the stalled surface front and possibly as far south as the Gulf, then moving north and overruning the cold dome of air, with a surface high typically found over the northern CONUS.

Model forecasts for these cases were more varied in their success as compared to the Alberta Clipper cases. Snowfall generally ranged from 1–4 in, but some events had embedded smaller areas of greater snowfall, such as 7–9 Feb when an area of 4–7 in of snow fell over eastern Kansas within a larger area of lighter snowfall. The most dramatic example of an embedded band occurred during the 28–30 Jan storm, with a narrow ~east-west band of 8–16 in snowfall across portions of Kansas. Perhaps the forecasts were more variable for these events because the forcing was at times more subtle than with the Alberta Clippers. While there was a little bit of overforecasting by the high-resolution models (for example, the 14–16 Feb storm), there was more of a tendency for all the models, including the operational models, to miss some of the heavier areas of snow. This is most apparent for the 28–30 Jan storm, but it occurs in others as well (see Table 2). As with the Alberta Clipper cases, neither the ARW nor the NMM was dramatically superior to the NAM model in terms of overall snowfall predicted. The GFS, as with the other cases, tended to have a more broad-brushed precipitation forecast.

3.3 *Nor'Easters*

The most intense winter storms in terms of a surface low development and often snowfall were the Nor'Easters. The 2004–2005 winter was a prolific one for coastal storms, with record snowfall over portions of the Northeast. We saved data for three of these storms, with the 1 Mar storm shown in more detail in Section 4. As noted above, coastal storms often occurred as the systems discussed earlier reached the East Coast (23–24 Jan and 10–11 Feb), though they could develop separately (1 Mar). A composite of snowfall for the three cases is shown in Fig. 3. At least for our sample of three of the Nor'Easters, the forecasts from the ARW and NMM were generally good, but they were not notably superior to the operational NAM in terms of forecasts of total snowfall. One somewhat different aspect was the more agressive predictions of precipitation minima and maxima associated with the interaction with terrain by the NMM and ARW. While this is also found in the NAM, it is even more notable in the ARW and NMM, as would be expected with their higher horizontal grid resolution. The strong orographic influences appeared to result in good overall snow forecasts for the 23–24 Jan case, but tended to be somewhat overdone in the 1 Mar case. Although orographically enhanced snowfall is not the main subject of this paper, it generally cannot be ignored in the case of Nor'Easters. We have also noted a tendency to overpredict orographic snowfall when examining cases in the Colorado Rockies, and a similar conclusion was noted by Tardy et al. (2005)

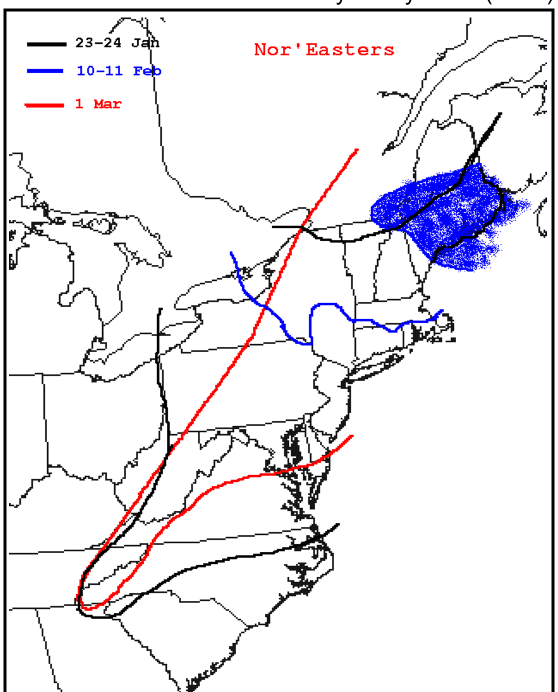

Fig. 3. Snowfall distribution for the three Nor'Easter cases. Shading for the 10–11 Feb case denotes snowfall greater than 12 in.

in their evaluation of the NMM and ARW for the Salt Lake City WFO area.

Two other cases are listed in Table 1 that did not fall into the three main categories, the 6–7 Feb case of a band of snow at the back edge of the precipitation shield associated with a stalled cold front, and the 19–21 Feb case where a well-defined surface low develops east of the Rockies and moves into the Midwest. Both cases are summarized in Table 2.

4. DETAILED CASE STUDIES

Two of the cases studied are discussed in greater detail in this section. Part of the motivation for presenting more specific details is to better demonstrate the kind of structures that a high-resolution model is capable of resolving. This can be demonstrated best by comparing output of model reflectivity, a field not available currently from the operational model suite, with observed reflectivity. How well are the models able to capture some of the structures within the storms, and is the timing and location accurate enough to be of value for forecasters? Does such accuracy, if present, extend as far in advance as a 36 to 48 h forecast, since one of the unique aspects of the DWFE was to extend a high-resolution model forecast out to 48 h. The general conclusion obtained by examining the snowfall for the various cases was that there was no significant difference in snow accumulation forecasts, overall, between the high resolution models and the operational NAM, at least for the types of large-scale systems considered here. The question then is whether there is added value for operational forecasting in the timing, location, and behavior of significant smaller scale bands within the overall snowfall.

4.1 *1 Mar Nor'Easter*

This case demonstrates the ability of both WRF models (the ARW and NMM) to predict rather well the snowbands associated with one of a large number of snowstorms that affected the New England area during the winter of 2004–2005. At the same time, this case illustrates how the two WRF models were closer in appearance to each other than they were to the actual radar observations – something seen repeatedly during the DTC Winter Forecast Experiment. This suggests that the initial and boundary conditions provided by the NAM model were more influential in producing mesoscale structures than were the details of the numerics and physics in the two models.

Although the amount of snow that fell during the 28 Feb–1 Mar 2005 storm was not impressive by New England standards, being generally in the range of 4–10 in (10–25 mm) over a 24-h period (Fig. 4a), the mesoscale structure of the snow was striking. Both WRF models predicted storm total snow amounts approximately correctly, though the distribution had a tendency to be somewhat too influenced by the local topography. The highest amounts were predicted over the more mountainous regions of the Adirondacks in eastern New York state, the Berkshires in Massachusetts, and the Green Mountains in Vermont (Fig. 4b), whereas comparison with the observed amounts in Fig. 4a suggests a more diminished topographic influence occurred in nature. However, much less mesoscale structure was evident in the NAM forecasts of total precipitation over New England over the storm's history (Fig. 4c).

A more detailed analysis of the morphology of the snowbands during the most active part of the storm is provided in Fig. 5, which shows 3-hourly displays of composite reflectivity fields. The most coherent, long-lasting, and strongest of the snowbands was A, which propagated northward and then northwestward as the storm system developed off the East Coast. Bands B and C propagated transversely to the dominant southwesterly flow aloft, and seemed to converge into a single mass soon after 0900 UTC. Band D was the most prominent of the bands, but formed later in the lifecycle of the storm; it also was a transverse band. Thus, 3 of the 4 bands had the character expected of gravity waves, similar in appearance to precipitation bands seen in other strong winter storms affecting this region (e.g., Bosart and Sanders 1986; Zhang et al. 2001). Evidence is presented below that no significant temperature gradient supportive of either frontogenesis or conditional symmetric instability (CSI) was present in the vicinity of these bands.

A comparison between the simulated reflectivity fields forecast by the ARW and NMM models at the same 3-hourly intervals as in Fig. 5 is presented in Figs. 6a and 6b, respectively. The NMM model displays a tendency to exhibit greater coverage of reflectivity < 25 dBZ. This is the result of differences in the way liquid water and ice species are treated in the model microphysics schemes, particularly the assumed size distributions for snow (Koch et al. 2005b). Yet, the most striking thing is how similar the forecasts appear from the two WRF models, despite the fact that they use quite different numerics and physics schemes. In particular, the placement, orientation, and number of precipitation bands forecast by the two models are remarkably similar to one another. Comparison of these forecast band characteristics with the observed bands shows fairly good correspondence overall, particularly for bands A and D, but the details pertaining to the other two bands are only moderately well forecast (mainly the orientation of the bands).

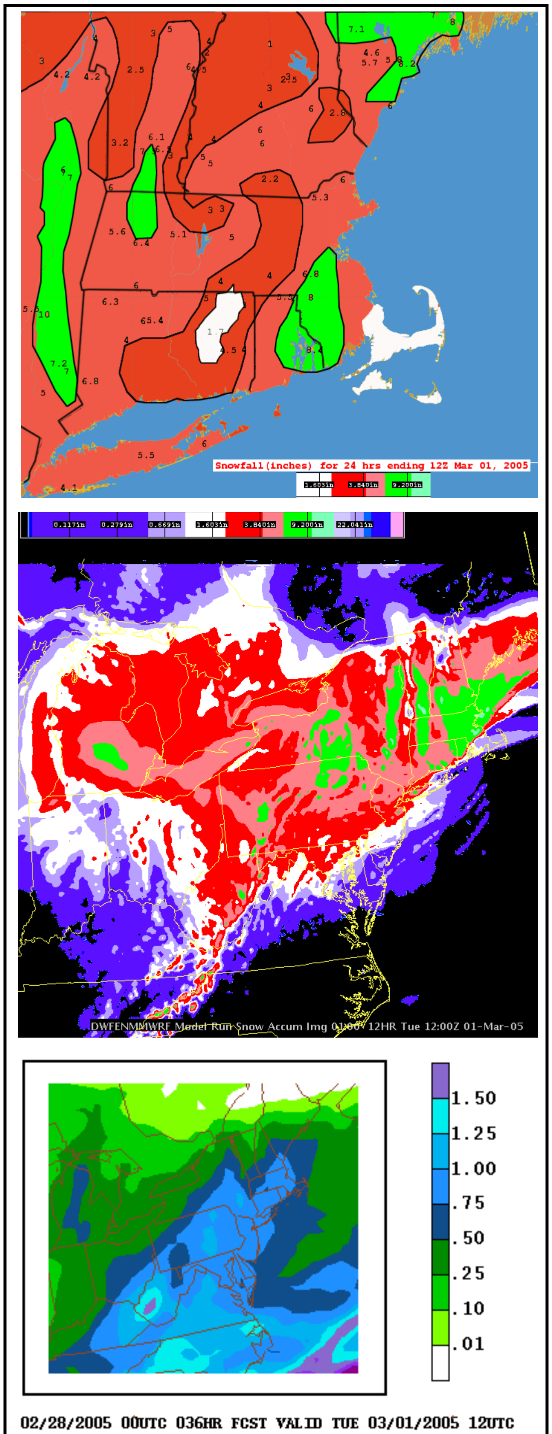

Fig. 4. Snow accumulations a, top) observed over 24-h period ending at 1200 UTC 1 Mar, b, middle) forecast for the 12-h period ending at the same time by the NMM model, in comparison with c, bottom) NAM forecast of total precipitation for the 36-h period. Although the two periods are not identical, nearly all of the observed snowfall occurred after 2200 UTC 28 Feb. Regions in red in panels a) and b) received < 4 in, those in pink received 4–7 in, and those in green > 7 in.

A chief advantage of the simulated reflectivity product appears to be that it allows one to more easily see detailed mesoscale structures capable of being forecast by finer resolution models, such as lake-effect snowbands, the structure of deep convection, and snowbands in winter storms. Three-hourly accumulated precipitation and mean sea level pressure fields forecast by the NMM model are displayed in Fig. 7, for comparison with the reflectivity fields in Fig. 6b. Clearly, the ability of accumulated precipitation fields to show useful mesoscale detail is quite limited. Note the existence of one additional band not labeled in Fig. 6 in western Pennsylvania and eastern Ohio. This band is directly associated with the surface cold front, which emanates from a vigorous low pressure system in the vicinity of Lake Erie. A classic secondary cyclone development is also obvious along the Eastern Seaboard. The center of this cyclone is forecast to deepen by the NMM model to 986 hPa by 1200 UTC 1 March (by comparison, the ARW model predicted a minimum pressure of 981 hPa).

Finally, we present some likely mesoscale mechanisms for the generation of the various snowbands in the WRF model forecasts. Band A was directly associated with strong warm advection and cyclonic vorticity at 700 hPa at all times (Fig. 8). Bands B and D were associated with significant disturbances in the wind field, propagating transverse to the flow, and were not found in the presence of any discernible horizontal temperature gradient at 700 or 850 hPa. Thus, such mechanisms as frontogenesis or CSI can be easily dismissed as being the cause. Gravity waves are a possible causative factor for bands B and D, except that no discernible disturbance is found in the MSLP field (Fig. 7). However, these bands could be associated with gravity waves in an elevated duct layer.

4.2 *18-19 March Alberta Clipper*

This storm was the third in a series of Alberta Clippers that began on 15 Mar, and by far the strongest, producing a record-setting snowstorm for parts of Minnesota and Wisconsin. The event was remarkable in that close to 2 ft of snow fell in about a 24-h period in the core of an overall very narrow band of snow. An overview of where the main band of snow fell can be seen from the 24-h NOHRSC snow water equivalent analysis in Fig. 9. The maximum precipitation for this 24 h period was in the 0.98 to 1.4 in category, stretching across southern Minnesota into western Wisconsin. Affected WFOs compiled storm total graphics for this event, with the one from the LaCrosse, Wisconsin, WFO in Fig. 10 and from the Minneapolis, Minnesota, WFO in Fig. 11. Maximum snowfall totals were just over 20 in over far southern Minnesota near the Iowa border to almost 2 ft eastward into western Wisconsin. The intensity of the snowfall was very impressive, with

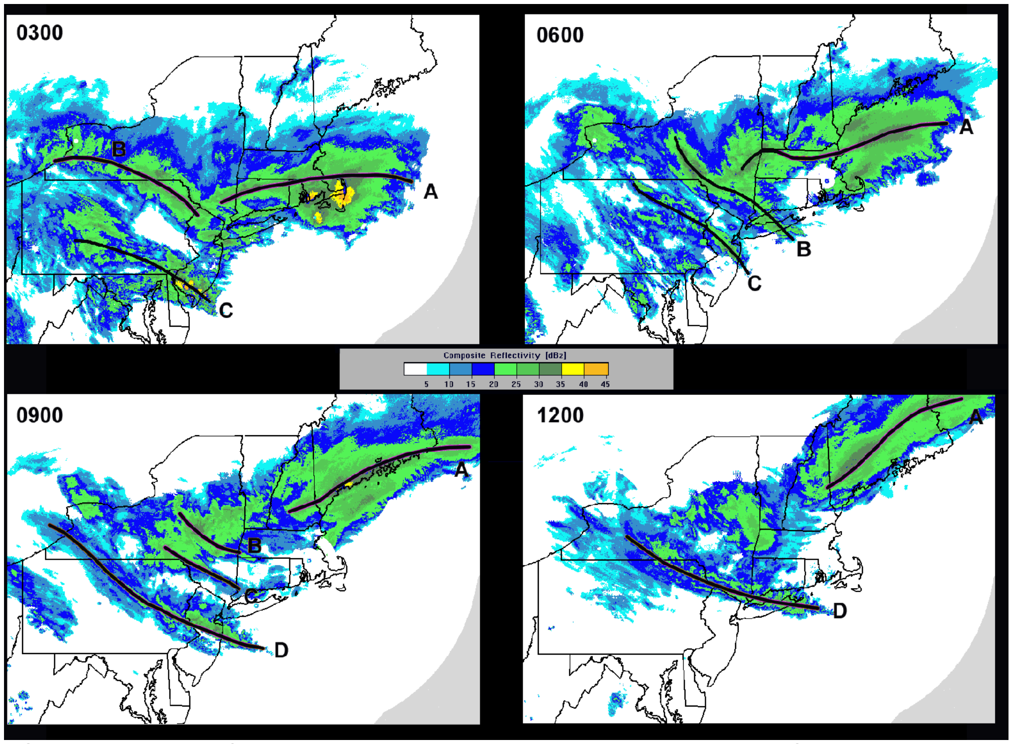

Fig. 5. Composite radar reflectivity displays at 0300, 0600, 0900, and 1200 UTC 01 March 2005 over New England (dBZ), showing snowbands A, B, C, and D, as determined from hourly displays. This highly quality-controlled national radar mosaic product is being produced experimentally by the National Severe Storms Laboratory and is available on a limited basis at the time of this writing.

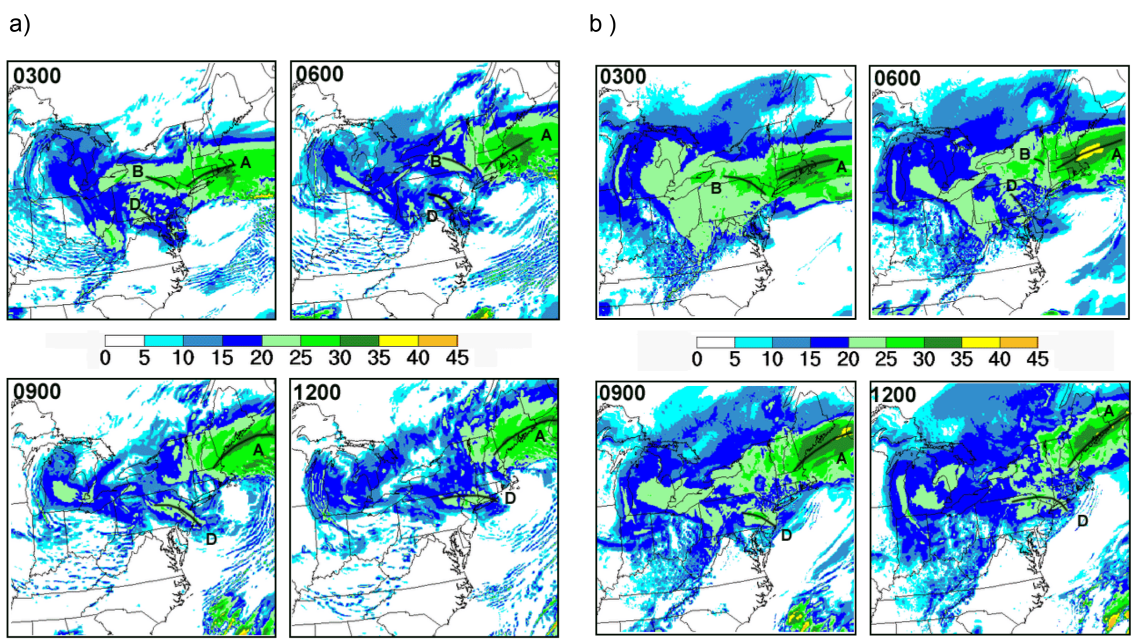

Fig. 6. Simulated composite radar reflectivity fields (dBZ) at 0300, 0600, 0900, and 1200 UTC 01 March over the northeastern U.S. forecast by a) the ARW model, and b) the WRF-NMM model, showing precipitation bands A, B, and D for comparison with the observed bands in Fig. 5.

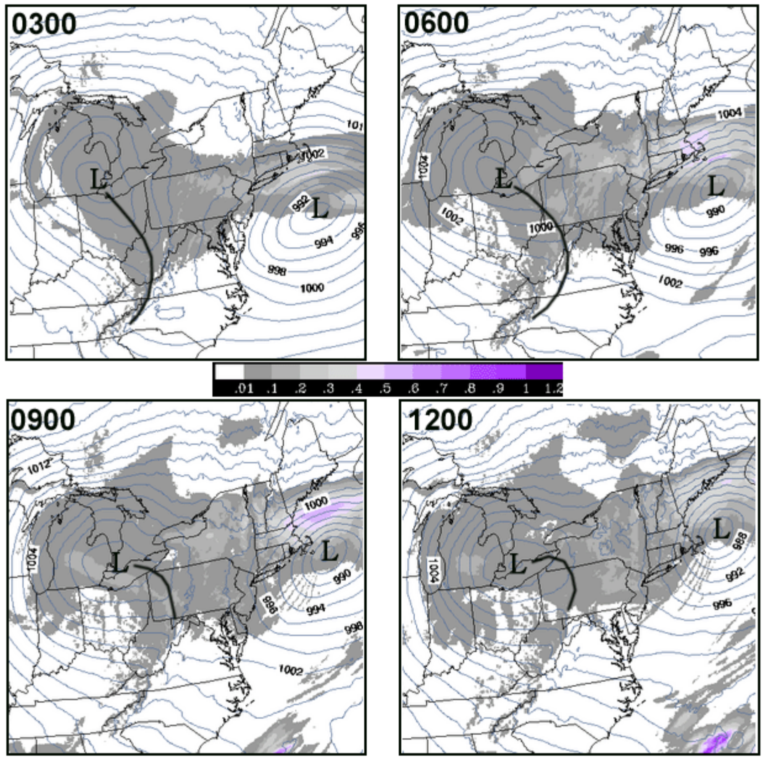

Fig. 7. Mean sea level pressure (2 hPa isobar intervals) and 3-hourly accumulated precipitation field (inches, see colorbar) forecast for 0300, 0600, 0900, and 1200 UTC 01 March by the WRF-NMM model. Dark line in eastern Ohio- western Pennsylvania represents forecast surface cold front.

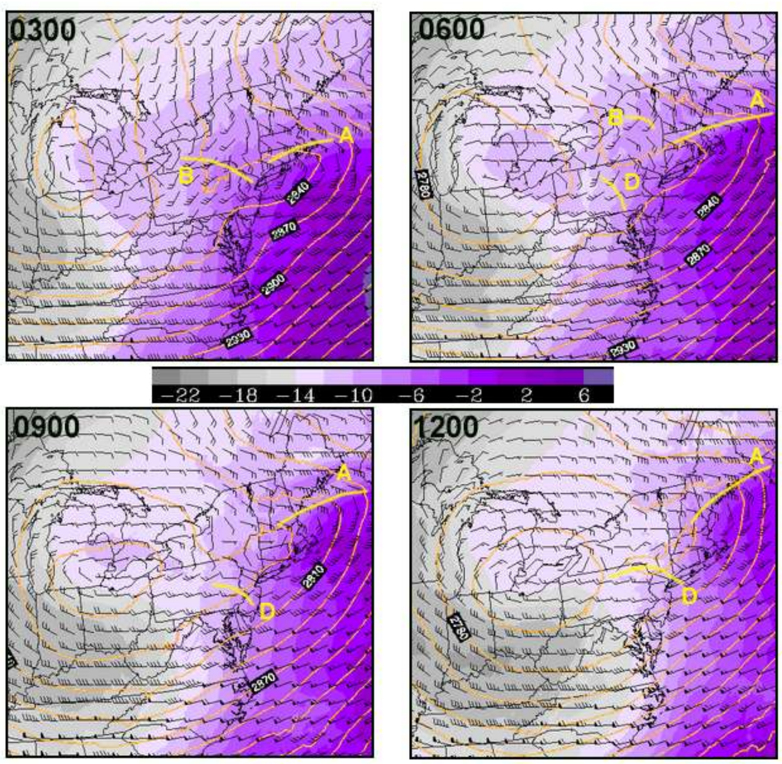

Fig. 8. Forecasts of winds (kt) and temperatures (C, see colorbar) at 700 hPa by the WRF-NMM model for 0300, 0600, 0900, and 1200 UTC 01 March. Precipitation bands forecast in the simulated composite reflectivity fields are overlain for comparison with Fig. 6b.

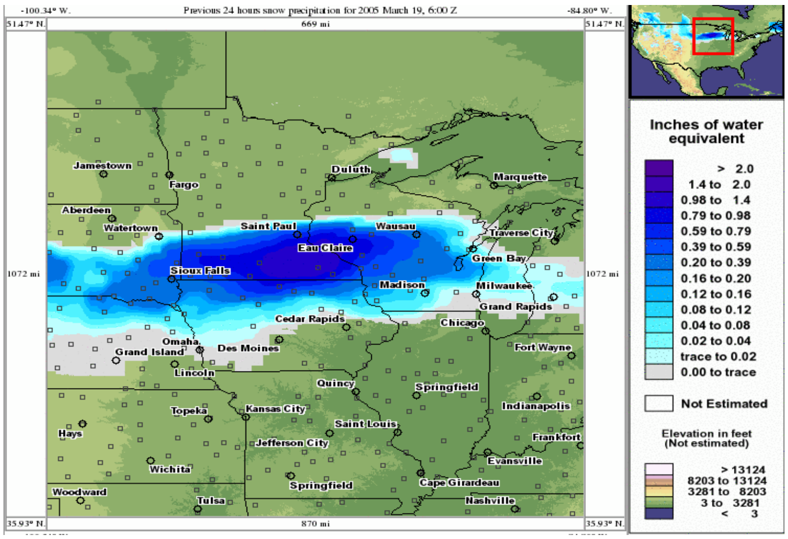

Fig. 9. NOHRSC 24-h snow precipitation analysis ending at 0600 UTC/19 Mar. Darkest blue = 0.98-1.4 in.

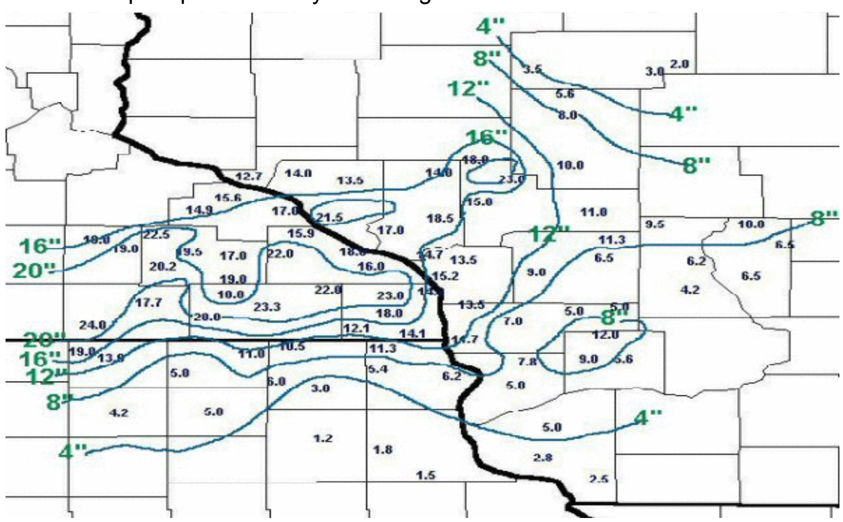

Fig. 10. Storm total snowfall, in inches, compiled by the LaCrosse, Wisconsin, WFO.

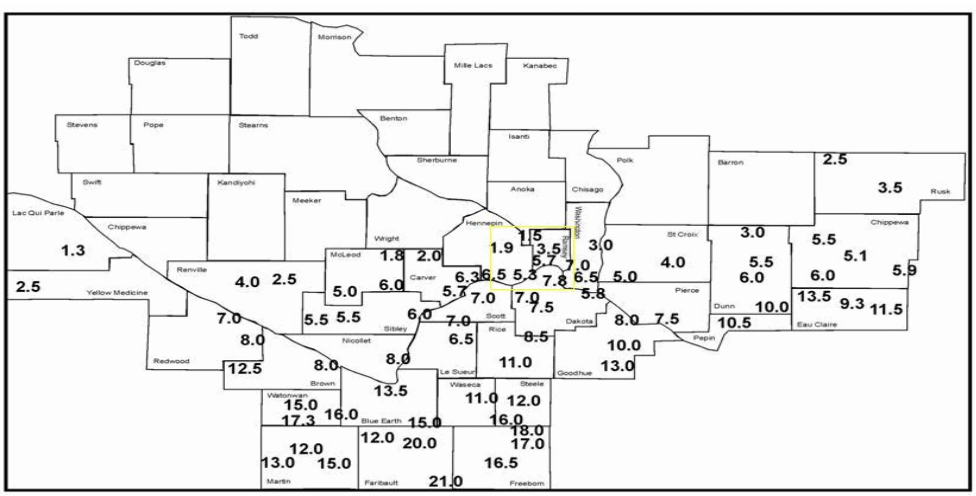

Fig. 11. Snowfall totals, in inches, for the 18–19 March storm compiled by the Minneapolis, Minnesota, WFO. The yellow box represents the approximate Minneapolis area.

Rochester, Minnesota setting an all time 24-h snowfall record of 16.8 in, while LaCrosse, Wisconsin, broke the daily snowfall record.

Another interesting feature of the snowband was the very sharp northern edge. The yellow box in Fig. 11 is the approximate outline of the greater Minneapolis area, illustrating how the snowfall just across the greater city area ranged from a dusting to over 6 in. The boundary between no snow at all and a significant accumulation was quite narrow, on the order of 20 mi (32 km) in the north-south direction. As the storm moved into Wisconsin on 19 Mar the snow distribution became more widespread, while the amounts decreased. In this section we focus on the portion of the storm that produced the remarkable east-west band of snowfall. The majority of the snow in the heavy band fell between 0000 UTC 18 Mar and 0000 UTC 19 Mar, though additional accumulations did fall over eastern portions of the band through about 1200 UTC 19 Mar. This timing of the snowfall makes it possible to examine longer range forecasts (~36 to 48 h) from the 0000 UTC 17 Feb runs, and contrast them with 0 to 24 h forecasts from the 0000 UTC 18 Feb runs. Such a relatively narrow band of heavy snow represents an excellent test for the high-resolution models.

An overview of the upper level and surface fields for this case is given in Fig. 12. A shortwave trough at 500 mb emerges out of western Canada and drops into Idaho and western Montana by 1200 UTC 17 Mar, but unlike the two previous systems during the week of the 17th this wave amplified as it approached the Midwest 24 h later. At the surface a stalled front lay across southern Iowa, westward into central Nebraska at 1200 UTC on 17 Mar, with the narrow band of snow associated with the second system in this series (discussed in Section 2) diminishing. A surface low develops along the frontal boundary as the upper level shortwave approaches, and by 1200 UTC 18 Mar it is centered near Omaha, Nebraska, with the front starting to lift northward over western Iowa as a warm front. The period of heaviest snows occurred over the next 12 h as the surface low tracked across Iowa, creating a narrow zone of intense lift that will be shown later in this discussion.

The first focus will be on how well the models did in forecasting the snowfall for this case. Were they able to capture this rather extreme event? Comparison of forecasts of both model predicted snow, using the AWIPS snow algorithm, and precipitation, will be made with observed amounts. We translated the snow reports into estimated precipitation, since there are considerably more snowfall observations than precipitation reports, in order to better compare to the precipitation forecasts. An appropriate snow to liquid was estimated by examining official NWS stations that recorded both. The following totals were found for this event, listed as total snow and total precipitation, both in inches, and the ratio of snow to liquid:

- Minneapolis, MN: 5.3/0.33/16:1
- Rochester, MN: 20.1/1.51/13.3:1
- LaCrosse, WI: 14.7/1.26/11.7:1
- Eau Claire, WI: 13.5/0.77/17.5:1

The average snow to liquid ratio for this event using these four stations was 14.6:1, quite a bit more than the "standard" 10:1 ratio. Applying the calculated ratio to the maximum snowfall of ~23 in gives a liquid accumulation of 1.58 in. Our estimation then for precipitation within the heaviest part of the band would be around 1.5 in, about 0.20–0.30 in higher than the NOHRSC estimate.

Forecast comparisons for the two initialization times of interest are shown in Fig. 13, for 48-h forecasts for runs initialized at 0000 UTC 17 Mar, and in Fig. 14, for 36-h forecasts for runs initialized at 0000 UTC 18 Mar. The most striking feature of all the forecasts is that all the models, from both initialization times, had a significant band of heavy precipitation located in the approximate area that it occurred. This is true of both the high resolution models and the operational models. A closer look first at the 0000 UTC 17 Mar runs from the NMM and ARW indicates that both have a maximum in the 1–1.5 in range across southern Minnesota into western Wisconsin, close to where it occurred. The area of maximum precipitation is larger for the NMM forecast, and it has higher snowfall amounts, a maximum value in the 25–30 in range, compared to the 15–20 in range for the ARW. The lower numbers verify better so there was some overprediction of amounts in the NMM. The location of the main east-west band is similar in both forecasts, but the NMM has an area of quite heavy precipitation in eastern Iowa that is overdone and is not found in the ARW forecast. Both forecasts have a very sharp gradient at the northern side of the band. This gradient should lie east-west near Minneapolis, which is close to what is shown in the ARW forecast, while the NMM is shifted too far to the north.

The NAM 48-h total precipitation forecast from 0000 UTC 17 Mar is also shown in Fig. 13. Maximum values are lower than both the ARW and NMM, though the maximum that is shifted east to near the Wisconsin/Minnesota line is in the range of the observed maximum precipitation. The NAM forecast shows a sharp northern gradient also, and it lies in the vicinity of the Minneapolis area. The GFS forecast (Fig. 13) is broader, as would be expected owing to its coarser resolution, with a lower maximum value and an orientation to its precipitation "area" that is off somewhat. Still, even the GFS had a small maximum of precipitation in the correct area in southeast Minnesota.

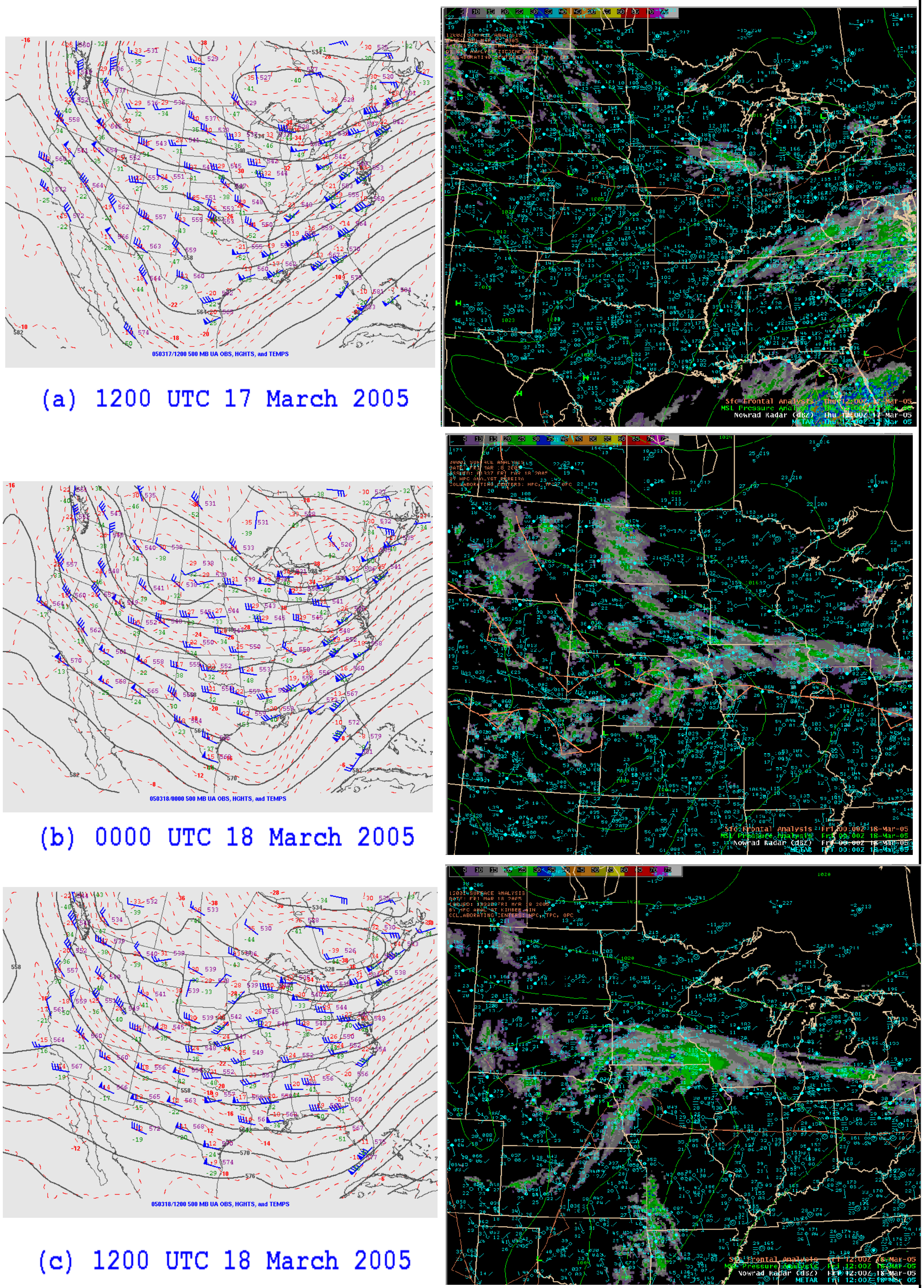

Fig. 12. Overview of the 18 March case. 500 mb plot and analyses on the left, surface METAR plot with pressure analysis and nowrad radar on the right, for (a) 1200 UTC 17 Mar, (b) 0000 UTC 18 Mar, and (c) 1200 UTC 18 Mar.

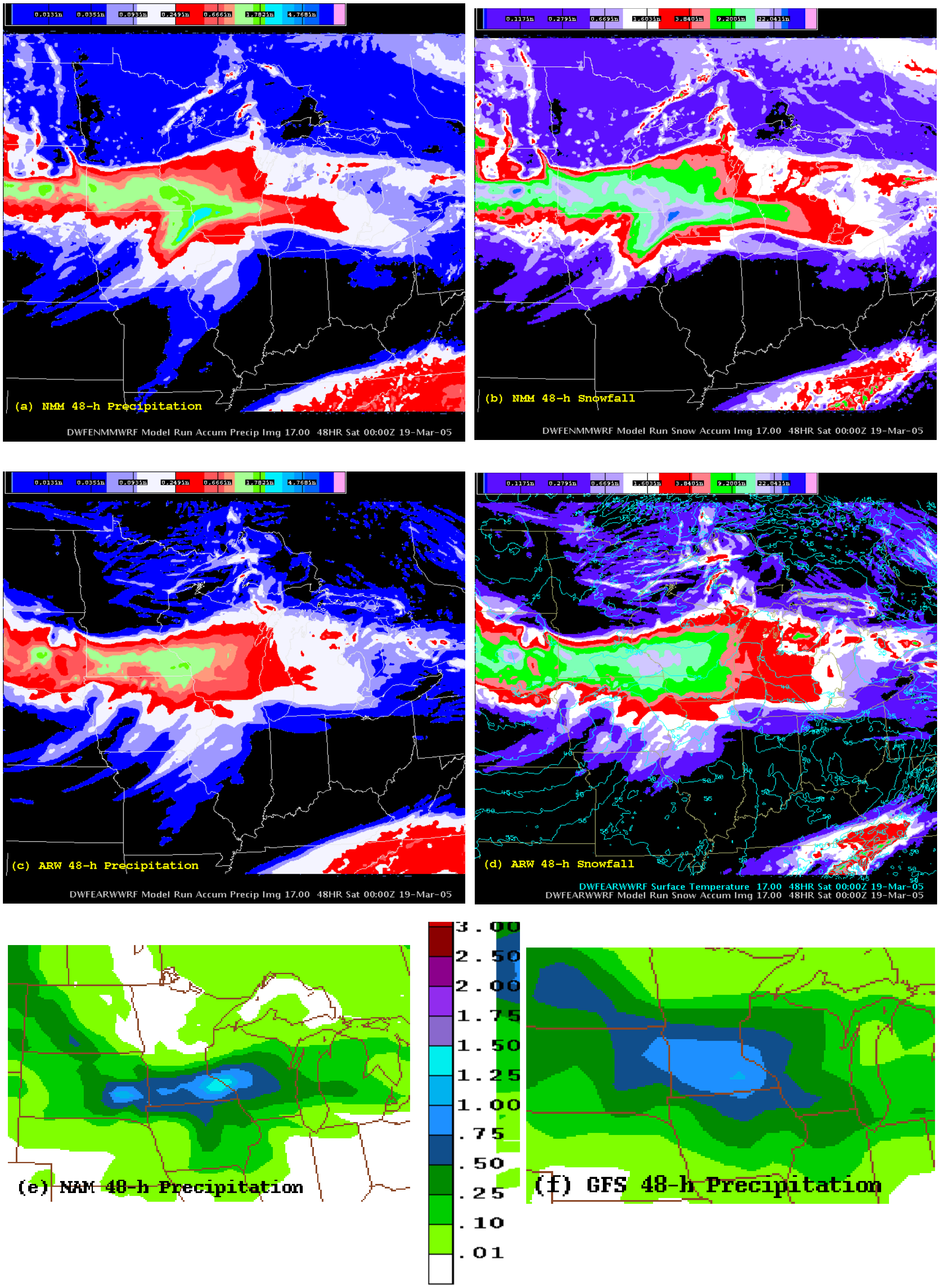

Fig. 13. 48-h forecasts from the 0000 UTC 17 Mar runs, ending at 0000 UTC 19 Mar. NMM top row, ARW middle, with accumulated precipitation (in),.left column, and accumulated snow (in), right. In the bottom row is the accumulated precipitation from the NAM (left) and GFS (right), with the scale in the middle.

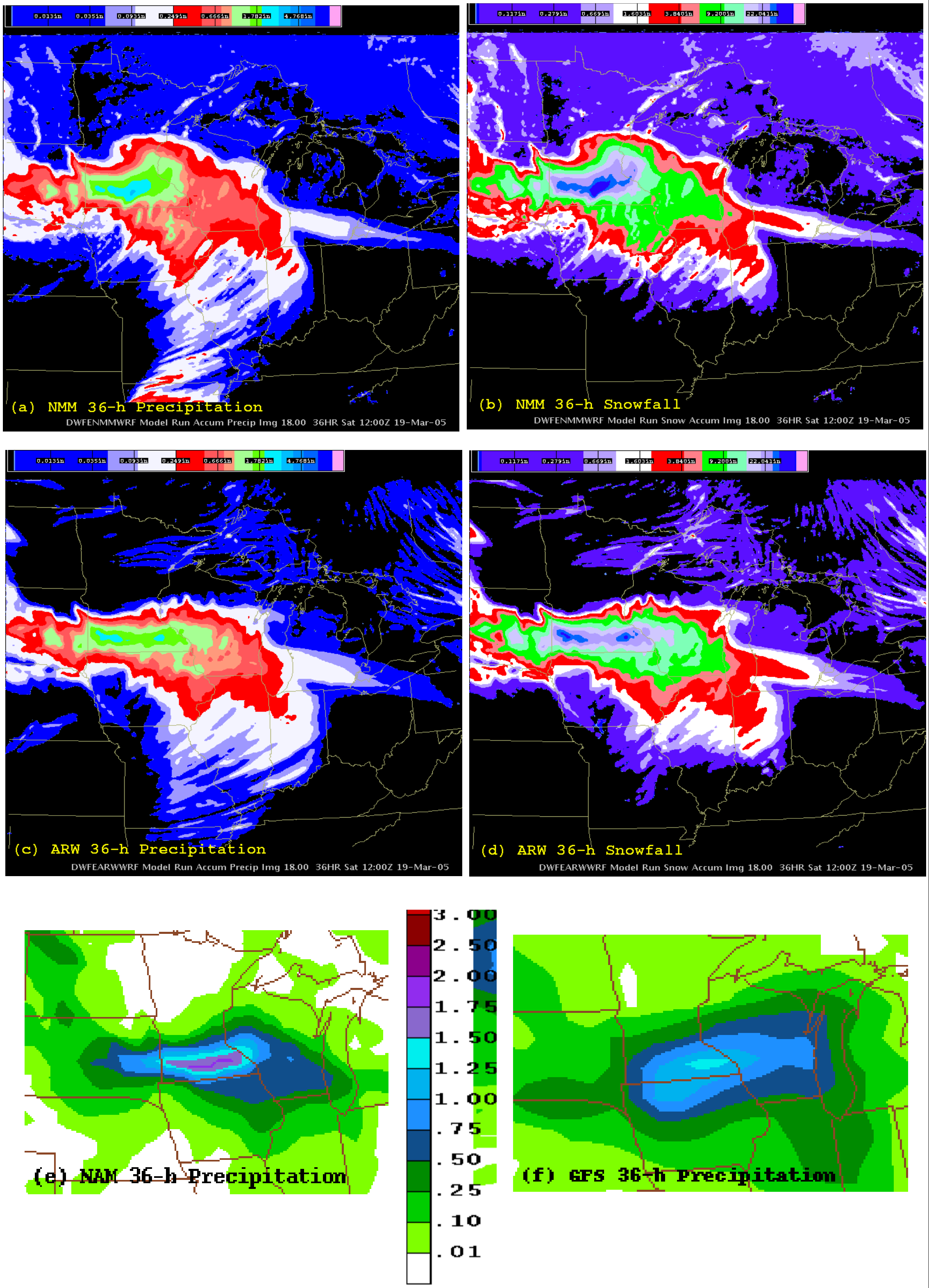

Fig. 14. As in Fig. 13, except 36-h forecasts from the 0000 UTC 18 Mar runs, ending at 1200 UTC on 19 Mar.

The timing of the snowfall enables one to examine if there were any substantial improvements for forecasts made 24 h later. One difference with all the runs is that more precipitation is forecast, but this in part would be because some snow continued to fall after 0000 UTC 19 Mar that was not in the forecasts initialized at 0000 UTC on 17 Mar. Comparing these forecasts to the total snow and precipitation that fell shows that both high resolution models tended to predict too great a maximum snowfall, again more so for the NMM. The NMM had a maximum snowfall of over 30 in and precipitation over 3 in, with the maximum located too far to the west. The ARW had a couple of spots with over 3 in of precipitation and about 30 in of snow, but the area covered by this higher precipitation was smaller, and the location was for the most part closer to where the maximum snow fell. Both models tended to predict the maximum precipitation extending too far to the west across southern Minnesota. The NAM forecast showed a remarkably narrow band of maximum precipitation in the 1.75 to 2 in range, somewhat high, but located about where the axis of maximum snow fell across southern Minnesota. The GFS was consistent in keeping its precipitation maximum over southeast Minnesota, a good forecast, with amounts in the 1.25–1.5 in range, although the overall precipitation area was too spread out.

In terms of the sharp northern precipitation gradient, the NAM, ARW, and NMM all had a sharp gradient in about the right position, except again the NMM was way too far north with the northern edge to the precipitation in eastern Minnesota, even more so than from the previous days forecast. The GFS tended to smooth out the gradient on the northern end of the snowband.

The above comparisons indicated that the NAM model was hard to beat for the forecast of this narrow band of heavy snow, seemingly a tough forecast problem given the small area of snow and climatologically rare nature of the amounts. This conclusion is similar to what was found when examining most of the cases from the DWFE period. However, as the discussion of the 1 Mar Nor'Easter demonstrated, there are other aspects of the forecasts from the ARW and NMM, besides total snowfall, that are not available from the NAM and of potential use to forecasters, notably the temporal evolution of individual snowbands as seen in the simulated radar reflectivity fields. Next we will conduct a similar examination of other ARW and NMM fields for this case, concentrating on how the reflectivity forecasts compared to observed reflectivity.

A comparison of the ARW and NMM forecast reflectivity with observations is shown in Fig. 15 for the 1200-1800 UTC 18 Mar time period. In this figure we are able to compare 36- to 42-h forecasts of reflectivity from the 0000 UTC 17 Mar runs with 12- to 18-h forecasts from the runs 24 h later. Various bands identified in the radar observations are labeled in Fig. 15, with their counterparts labeled in the model reflectivity. Some of the points noted with the 1 Mar Nor'Easter case apply here as well: the NMM reflectivity forecasts have more structure and higher values than the ARW, and in general the ARW and NMM predicted reflectivity bands are more similar to each other than to observations.

As might be expected given the pattern of snowfall, an east-west band of reflectivity across southern Minnesota into western Wisconsin dominated the structure of this event. However, there were also more transient bands oriented ~north-south across Iowa during this same time. The main east-west band, labeled band “A” in Fig. 15, set up across southern Minnesota by ~0800 UTC 18 Mar, and persisted through much of 18 March. The first indications of the banding across Iowa began by 1100 UTC, growing to 3 distinct bands almost perpendicular to the main east-west band between 1100 and 1400 UTC. By 1800 UTC an additional ~north-south band (band E) developed in Iowa ahead of the other bands. It is clear from looping of the reflectivity imagery that maxima in reflectivity within the main band A often coincided with the intersection points with the other bands, and that bands B through E tended to be composed of small convective elements as opposed to the more uniform pattern of reflectivity exibited with band A.

Examination of the METAR observations and surface pressure analysis combined with the reflectivity image in Fig. 15 indicates that the main band, band A, is found in the cold air north of the warm front lying ~east-west across Iowa. At 1200 UTC 18 Feb the warm front is in southern Iowa, and lifts northward through the morning so that by 1800 UTC it is east-west across central Iowa. But despite the warm front moving ~150 km to the north in these 6 h, band A remains in place across southern Minnesota through 1500 UTC, and the northern edge only moves north ~50 km by 1800 UTC. The more north-south bands to the south of band A are more complicated and transient features. It appears that the most extensive of these bands, band D, is most closely associated with the cold front trailing the surface low in northwest Iowa, forming ~1000 UTC ahead of the cold front and remaining ~50-100 km ahead of the cold front thereafter. Although with the cold front, band D extends well north of the warm front and clearly intersects band A, suggesting there may be another mechanism also involved in producing this band, perhaps the same mechanism responsible for the other similarly oriented bands (B, C, and E), which do not appear to have any obvious surface-based forcing feature.

It is apparent from Fig. 15 that all the model forecasts captured the main band A, which was

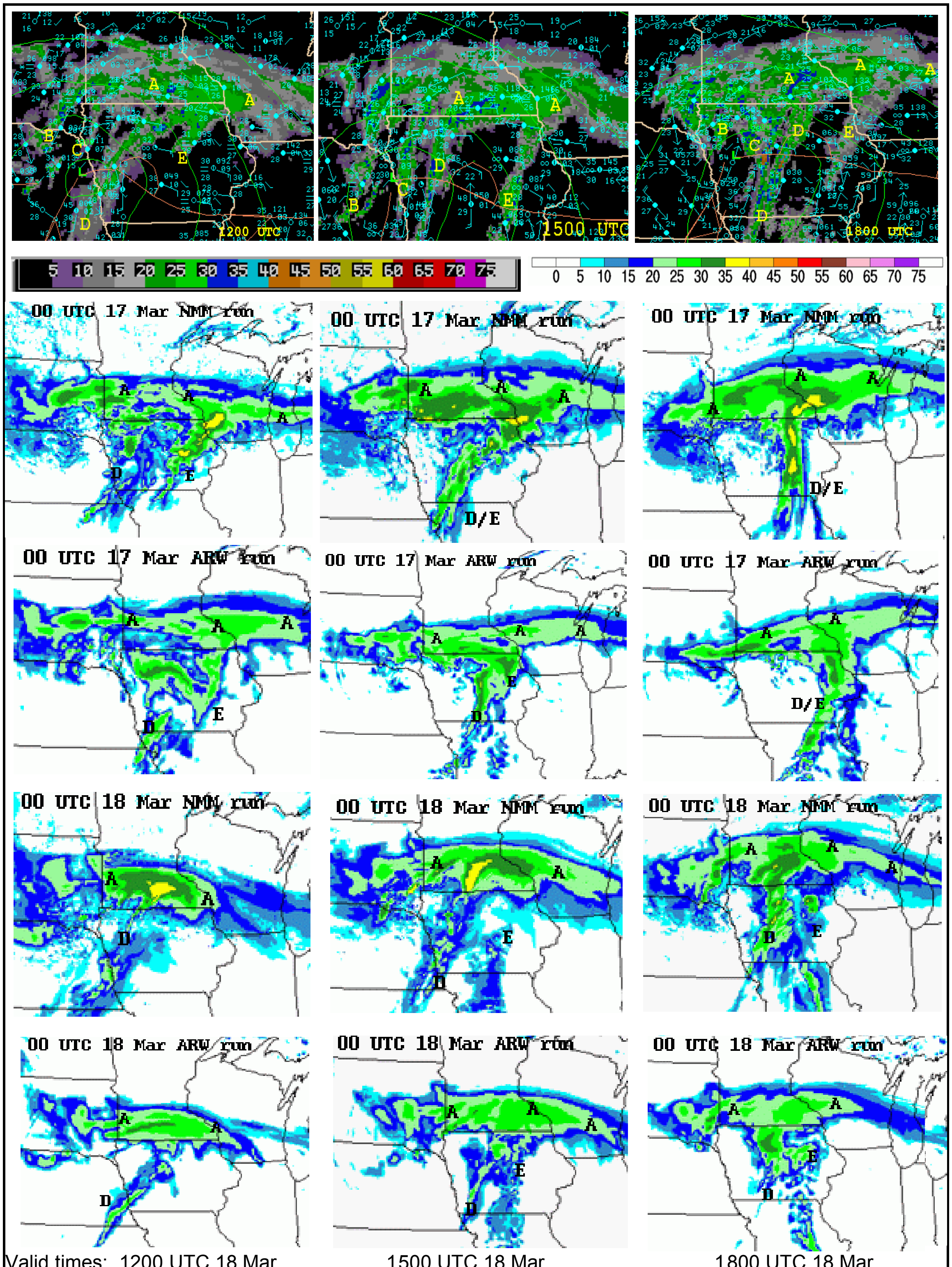

Fig. 15. Observed and model forecast reflectivity comparison. Times for the columns are 1200 UTC 18 Mar (left column), 1500 UTC 18 Mar (middle), and 1800 UTC 18 Mar (right column). Top row is observed reflectivity with METARs and pressure analysis. Other rows are the ARW and NMM forecasts of reflectivity from the 0000 UTC 17 Mar and 18 Mar runs, valid at the same times as the reflectivity observations. Letters denote identifiable bands (see text).

responsible for the heavy snow accumulations. There was less success in capturing the other bands, however, with the models mainly forecasting the band associated with the cold front, band D, and the one farther east, band E. Overall the 0000 UTC 17 Mar runs organized the bands south of band A more quickly than the runs on 18 Mar, and also predicted bands D and E to merge by 1800 UTC. Bands D and E did eventually merge, seen beginning to occur in Fig. 16 at 2100 UTC 18 Mar, so in this regard the forecasts from 0000 UTC UTC 17 Mar runs were about 3 to 6 h too fast but had the right idea.

It was noted that the NMM tended to have too much snow extending to the north of Minneapolis and eastward into western Wisconsin. Examination of the reflectivity forecasts from the 0000 UTC 17 Mar run suggest an overprediction of the intensity of the intersecting line (D/E) may be related to the excessive northward push of echo. The ARW is weaker with band D/E and keeps band A farther south, similar to what occurred. The reflectivity is pushed even farther northward on the 0000 UTC 18 Mar NMM run, even though bands D and E remain separate. The reflectivity forecast from the NMM valid at 1500 UTC shows what appears to be a strong extension of band D into band A, producing a 35 to 40 dBZ reflectivity maxima in south-central Minnesota. The 1800 UTC observed reflectivity image in Fig. 15 actually shows a similar feature, just to the right of the letter "A" in Minnesota, with maximum reflectivity in the 30 to 35 dBZ range. The same forecast from the ARW model has considerably weaker reflectivity and does not have the ~north-south reflectivity maxima into Minnesota. Interestingly, then, the NMM may have better captured some of the very small scale reflectivity structures than the ARW, but may have been too strong with the intersecting line.

Wind forecasts at 850 mb for 1800 UTC 18 Mar from both 0000 UTC 18 Mar runs are compared in Fig. 17, and it is apparent that the NMM had a much more southerly flow into band A midway across the southern Minnesota border than did the ARW. This more southerly flow would have pushed the warmer and moist air farther to the north and led to too much precipitation north of Minneapolis.

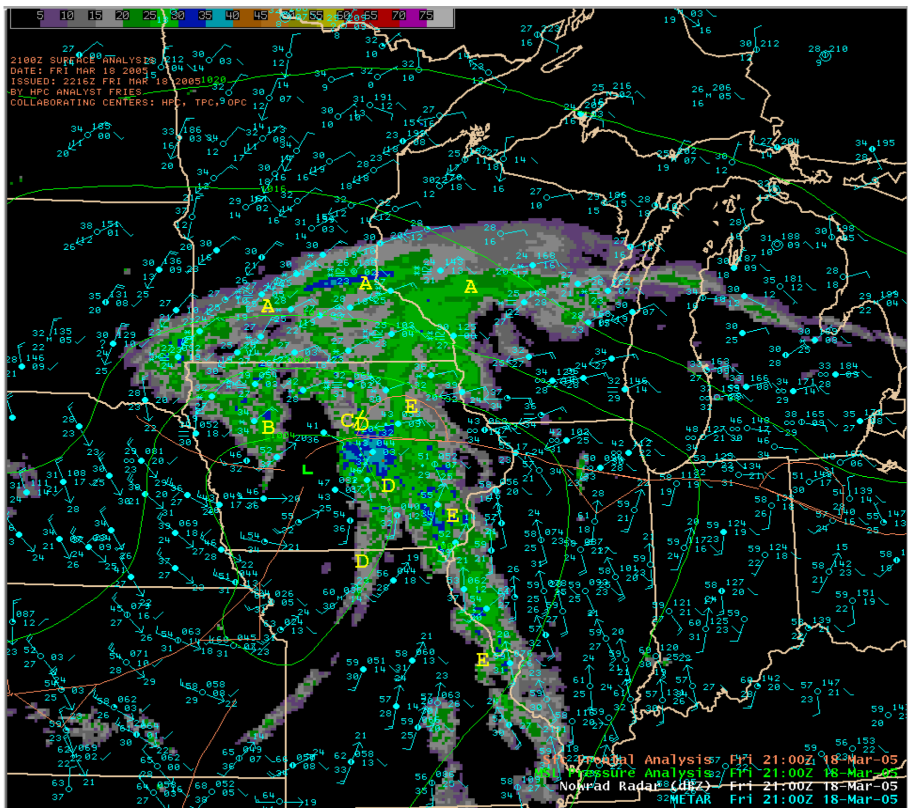

Fig. 16. Radar reflectivity with METARs and surface pressure and front analyses for 2100 UTC 18 Mar.

In terms of forcing for the bands, strong warm advection confined to a narrow area appeared to be the main forcing for the east-west band A. This is seen by examination of a cross section across the band, shown for the ARW and NMM in Fig. 18. The cross section for both models is aligned approximately perpendicular to the band as it was positioned at 1200 UTC. Both models forecast a concentration of low-level warm advection coincident with band A. The slope of the

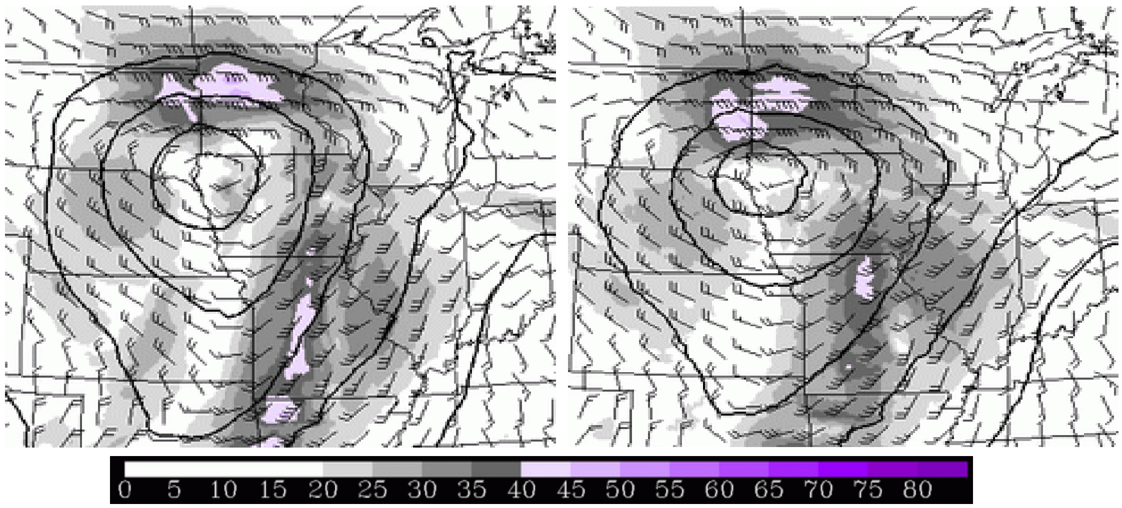

Fig. 17. 850 mb wind (knots, with color coded by speed according to the scale) and height (m) forecasts from the NMM (left) and ARW (right) for 1800 UTC 18 Mar.

equivalent potential temperature lines is steeper in the ARW forecast, with a more vertically erect concentration of warm air advection. The more shallow slope to the low-level baroclinic zone, coupled with a stronger component of southerly flow forecast by the NMM at low levels, likely accounts for the excessive spread of snow to the north.

The cause of the multiple ~north-south bands, as noted earlier, is not as apparent. These bands do occur in the vicinity of a small jet streak that is identifiable in the ARW and NMM 300 mb forecasts (not shown), suggesting gravity waves as a potential mechanism.

In summary, the NMM and ARW model precipitation forecasts were generally similar to each other and also to the NAM. In fact, snow precipitation forecasts by all the models, including the GFS, showed skill in predicting a record-breaking snowfall event over a small area as far as 48 h in advance. Such similarity may point to the importance of initial conditions rather than model physics in determining the snowfall for this case. However, it is important to note that the greater numerical precision of the WRF modeling infrastructure and higher resolution of the DWFE models as compared to the NAM, allowed depiction of fine scale features embedded within the precipitation shield. For instance, the NMM area of greater than 30 dBZ snowfall in southeast Minnesota at 1500 UTC 18 Mar. Although such features may not be observed at the exact time and location as forecast, explicit forecasts of the *character* of the precipitation shield alert forecasters to the possibility of such heavy snowfall (as was observed in this case). Similar advantages to high-resolution models have been noted by Roebber et al. (2002, 2004) for warm season convective events.

5. CONCLUDING REMARKS

The DTC DWFE occurred during a very active winter period from January through March 2005, allowing for an evaluation of forecasts for a number of different storms. We concentrated on events that produced a significant swath of snow across a large area.

Comparison of forecasts from the two high-resolution models with observed snowfall indicated that the models, overall, did a good job of capturing the events. When errors did occur they were not necessarily the same for both models, suggesting there may be some value in running an ensemble of models with different characteristics. We also compared the snowfall forecasts with forecasts from the operational NAM and GFS. We did not find any one case where the ARW or NMM were vastly superior to the NAM forecasts in terms of storm total snow precipitation. A number of reasons were suggested for this, including the fact that the ARW and NMM were initialized from the NAM, and that the 12-km horizontal grid resolution of the NAM sufficiently resolves the widespread winter systems studied here. Koch et al. (2005) show examples of smaller scale and convectively dominated systems, such as lake effect narrow snowbands, where the ARW and NMM with higher resolution and explicit convection can provide better forecasts than the NAM. The GFS overall tended to have broader areas of precipitation and compared less favorably to the other models in terms of details, though it usually forecast precipitation in the same area.

As noted in the case studies, the value of high resolution models for winter storms of the types studied here is in their ability to predict smaller

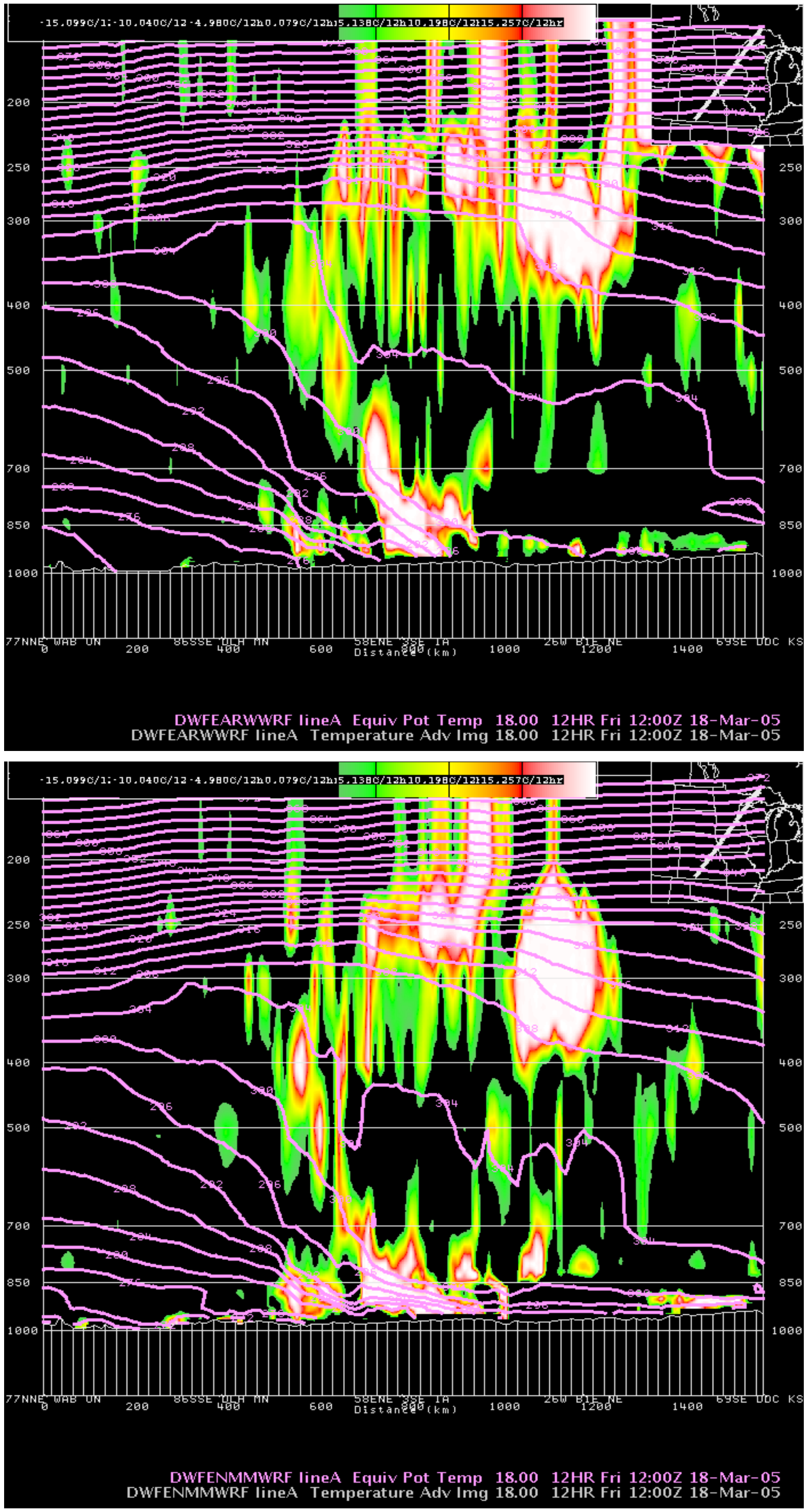

Fig. 18. Cross-sections from the ARW (top) and NMM (bottom) of 12-h forecasts of eqivalent potentia temperature (every 4ºK) and temperature advection (image, warm advection only), valid 1200 UTC 18 Mar.

scale structures within the storms. The use of simulated radar reflectivity as output from the models makes seeing such structures easier, and allows for direct comparison with observations in real-time. This should be of value for operational forecasters dealing with winter weather.

6. ACKNOWLEDGMENTS

We thank Nita Fullerton of FSL for a technical review of this manuscript and John Brown of FSL for an internal scientific review.

7. REFERENCES

Bernardet, L. R., L. B. Nance, H.-Y. Chuang, A. Loughe, M. Demirtas, S. Koch, and R. Gall, 2005: The Developmental Testbed Center Winter Forecasting Experiment. *21st Conf. on Weather Analysis and Forecasting/17th Conf. on Numerical Weather Prediction*, Washington, DC, Amer. Meteor. Soc., Paper 7.1.

Bosart, L. F., and F. Sanders, 1986: Mesoscale structure in the megalopolitan snowstorm of 11–12 February 1983. Part III: A large amplitude gravity wave. *J. Atmos. Sci.,* **43,** 924–939.

Demirtas, M., L. Nance, L. R. Bernardet, Y. Lin, A. Loughe, R. L. Gall, and S. E. Koch, 2005. Quantitative Precipitation Forecasts (QPF) verification of DWFE. *21st Conf. on Weather Analysis and Forecasting/17th Conf. on Numerical Weather Prediction*, Washington, DC, Amer. Meteor. Soc., Paper 7.2.

Koch, S. E., R. Gall, G. DiMego, E. Szoke, J. Waldstreicher, P. Manousos, B. Meisner, N. Seaman, M. Jackson, R. Graham, A. Edman, and D Nietfeld, 2005a: Lessons learned from the DTC Winter Forecasting Experiment. *21st Conf. on Weather Analysis and Forecasting/17th Conf. on Numerical Weather Prediction*, Washington, DC, Amer. Meteor. Soc., Paper 7.6.

Koch, S. E., B. Ferrier, M. Stoelinga, E. Szoke, S. Weiss, and J. Kain, 2005b: The use of simulated radar reflectivity fields in the diagnosis of mesoscale phenomena from high-resolution WRF model forecasts. *11th Conf. on Mesoscale Processes/32nd Conf. on Radar Meteorology*, Albuquerque, NM, Amer. Meteor. Soc (submitted).

Madine, S., N. Wang, E. Polster, J. Pyle, R. Brummer, 2002: FX-Net National: a nonlocalized internet-based meteorological workstation. *Interactive Symp. on the Advanced Weather Interactive Processing System (AWIPS)*, Orlando, FL, Amer. Meteor. Soc., J330-J332.

Roebber, P. J., D. M. Schultz, and R. Romero, 2002: Synoptic regulation of the 3 May 1999 tornado outbreak. *Wea. Forecasting*, **13**, 399–429.

——, D. M. Schultz, B. A. Colle, and D. J. Stensrud, 2004: Towards improved prediction: High-resolution and ensemble modeling systems in operations. *Wea. Forecasting*, **19**, 936–949.

Tardy, A., M. Jackson, and E. Szoke, 2005: Evaluation of high resolution model QPF performance in the complex terrain of the Great Basin as part of the DTC Winter Forecast Experiment. *21st Conf. on Weather Analysis and Forecasting/17th Conf. on Numerical Weather Prediction*, Washington, DC, Amer. Meteor. Soc., Paper 7.4.

Zhang, F., S. E. Koch, C. A. Davis, and M. L. Kaplan, 2001: Wavelet analysis and the governing dynamics of a large-amplitude mesoscale gravity wave event along the East Coast of the United States. *Quart. J. Roy. Meteor. Soc.*, **127,** 2209-2245.